Arch. Metall. Mater. **63** (2018), 3, 1257-1266

DOI: 10.24425/123799

A. KAJZER*#, K. RABIJ*, M. BASIAGA*, K. NOWIŃSKA**, M. KACZMAREK*,
T. BOROWSKI***, T. WIERZCHOŃ***

INFLUENCE OF STERILIZATION AND EXPOSURE TO THE RINGER'S SOLUTION ON MECHANICAL AND PHYSICOCHEMICAL PROPERTIES OF NITROCARBURIZED 316 LVM STEEL

Studies on biocompatibility of AISI 316LVM steel indicate the need to eliminate the nickel from the surface and replace it with other elements of improved biocompatibility. Therefore, in the presented work selected physicochemical and mechanical properties of the diffusive nitrocarburized layer formed by plasma potential by means of an active screen made of the Fe-Cr-Ni were studied.

In the paper we present results of microstructure and phase composition of the layers, roughness, and surface wettability, potentiodynamic pitting corrosion resistance, penetration of ions into the solution as well as mechanical properties. The studies were conducted for the samples of both mechanically polished and nitrocarburized surfaces, after sterilization, and exposure to the Ringer's solution.

Deposition of the nitrocarburized layer increased the contact angle, surface roughness, surface hardness, and corrosion resistance with respect to the polished surfaces. The nitrocarburized layer is a barrier against the ions release into the solution and sterilization and exposure to Ringer solution.

The obtained results showed beneficial increase of both mechanical and electrochemical properties of the deposited layer, and thus the applicability of the proposed method of surface treatment of the 316LVM steel for short-term implants after sterylization.

Keywords: AISI 316LVM steel; nitrocarburizing process; mechanical and physico-chemical properties

1. Introduction

Austenitic steels are widely used in medical implants, and medical instruments [1,2]. For these steels biocompatibility is essential. Biocompatibility is directly influenced by mechanical and electrochemical properties and surface wettability related mainly to its topography and chemical composition. The selection of functional properties of the steel for specific applications is mainly based on: the design of the product, the applied operation technique, time of use, as well as biomechanical characteristics of reconstructed tissues and their physicochemical properties [3]. Proper selection of chemical composition ensures high ductility and high strength, and paramagnetic structure, and primarily, one of the best corrosion resistances, especially to intergranular and pitting corrosion, of all steel grades [4].

Implants made of this steel when adjusted to the anatomical curvatures of bones and bone fractures may be exposed to mechanical damage of the surface. Interruption of the passive layer protecting the implant against the tissue environment can lead to reduction of corrosion resistance [5,6]. Therefore, it seems that the processes of electrolytic polishing and passivation do not always provide a surface with adequate hardness and abrasion resistance.

Increase of the corrosion resistance, and surface hardness as well, can be obtained by surface treatment [7-11]. More and more often processes of plasma or gas nitriding, or ion implantation are used [12,13]. Recently also the process of glow discharge nitrocarburizations is used. The mentioned technology combines the process of low-temperature nitriding and carburization in a low-temperature plasma, in which, next to a mixture of nitrogen and hydrogen, a methane is used [14].

This process enables the production on the austenitic stainless steel a double layer of nitrogen austenite γ_N and carbon austenite γ_C. Application of the modified process realized with the use of the active screen allows to process complex shape parts [15-17], which is especially important for medical instruments and implants. This technology allows for keeping a certain surface roughness, due to the reduction of the sputtering effect, resulting in improved mechanical and corrosion properties of these layers. Improvement of the 316LVM steel quality should be focused on shaping the structure of the surface layer. The whole process of surface modification shoul also include sterilization. Therefore, the aim of the study was to investigate the influence of the nitrocarburizing process carried out in the low temperature plasma using the active screen at 440°C on the structure and properties of the 316LVM steel.

* SILESIAN UNIVERSITY OF TECHNOLOGY, FACULTY OF BIOMEDICAL ENGINEERING, 40 ROOSEVELTA STR., 41-800 ZABRZE, POLAND
** SILESIAN UNIVERSITY OF TECHNOLOGY, FACULTY OF MINING AND GEOLOGY, 2 AKADEMICKA STR., 44-100 GLIWICE, POLAND
*** WARSAW UNIVERSITY OF TECHNOLOGY, FACULTY OF MATERIALS SCIENCE AND ENGINEERING, WOLOSKA 141 STR., 02-507 WARSZAWA, POLAND

Corresponding author: Anita.Kajzer@polsl.pl

2. Material and methods

2.1. Preparation of samples

In the study the 316LVM stainless steel in the form of discs with the diameter of d = 14 mm and the thickness of g = 3 mm was used. All samples before modification were ground on sandpaper of 800 and 1200 grit and polished mechanically using diamond suspension of 3 μm and 1 μm, and then polished using silicon oxide on the automatic polisher – Struers Tegramin-30. The prepared samples were subjected to the glow discharge plasma assisted nitrocarburizing using the active screen made of the Fe-Cr-Ni [13]. The nitrocarburizing process was carried out at 440°C for 21.6 ks. The pressure in the working chamber was equal to 200 Pa. The composition of the working mixture was as follows: N_2 and H_2 in the ratio of 1:3, and CH_4, which comprised 5% of the gas mixture volume. Prior to testing, all samples were cleaned in the ultrasound bath for 10 minutes in 96% ethanol. The samples were then divided into the following groups: I – mechanically polished, II – mechanically polished and steam sterilized, III – mechanically polished, steam sterilized and exposed to Ringer's solution. The same division was used for the samples with the surface layers IV, V – after steam sterilization and VI – after sterilization, and exposure to Ringer's solution. The steam sterilization was carried out using the HM260F autoclave (HMC EUROPE) at T = 135°C at time t = 60 min. and pressure p = 210 000 Pa. To simulate physiological conditions the samples of the group III and VI were kept in the Ringer's solution of the following composition: 8.6 g sodium chloride, 0.3 g potassium chloride, 0.48 g of calcium chloride in 0.001 m^3 of demineralized water. The samples were kept for 28 days at 37°C in the laboratory incubator 53 FD (BINDER).

In order to assess the influence of both, steam sterilization and exposure to the physiological medium, on mechanical and physico-chemical properties of the steel, the following tests were carried out: electrochemical, topography, morphology, surface wettability and mechanical ones.

2.2. Microstructure of the layer

Surfaces of the samples for microstructure observation were polished with SiC abrasive papers up to # 1200 grit, and then polished with diamond paste 1 mm. Etching of the the 316L steel was realized with the use of a reagent consisting of: 50% HCl +25% HNO_3 + 25% H_2O. The microstructure was observed using the optical microscope Nikon Eclypse LV150N. The phase composition of the produced layers after the nitrocarburising process of mechanically polished samples was determined using X-ray diffractometer Bruker D8 Advance using Cu Ka (λ = 0.154056 nm) radiation. The following parameters were applied: voltage 40 kV, current 40 mA, 2Q angle range from 37° to 55°, step D2Q – 0.05°, counting time – 3 sec.

2.3. Surface roughness

Due to the influence of the quality of surface preparation, corrosion resistance and the wettability of the surface, roughness measurements were conducted by means of the contact method, as recommended by the PN-EN ISO 4287: 1999 / A1: 2010 standard, with the use of the Surtronic S-100 profilometer (Taylor-Hobson). Measurements of the Ra and the Rz parameters were made for the total measured length equal to ln = 4 mm.

2.4. Potentiodynamic study

Study of pitting corrosion resistance was carried out by means of the potentiodynamic method using three electrodes: the reference electrode (saturated calomel electrode – SCE type KP-113), the auxiliary electrode (platinum electrode PtP-201 type), and the working electrode – the sample. The study was realized with the use of the VoltaLab PGP 201 potentiostat equipped with the Volta Master software. The study consisted in recording polarization curves in accordance with the recommendation of the PN-EN ISO 10993-15 standard. Corrosion tests started from indicating the open circuit potential E_{OCP}. Polarization curves were recorded from the initial potential $E_{init} = E_{OCP} - 100$ mV. The applied scan rate was equal to 1 mV/s. Once the anode current density had reached the value of 1 mA/cm^2, the direction of polarization was changed. On the basis of the obtained curves the following corrosion parameters were determined: corrosion potential E_{corr} breakdown potential E_b, repassivation potential E_{cp}, transpassivation potential E_{tr} and, using the Stern method, polarization resistance R_p. The studies were performed in the Ringer's solution at the temperature of T = 37 ±1°C.

2.5. Ion release study

In order to assess the amount of ions released to the Ringer's solution, tests of metallic ions permeability were performed. The testing was performed for the samples from the I, II, IV and V group. The amount of Fe, Si, Cr, Ni and Mo ions released to the solution was designated. Each sample was placed for 28 days in 100 ml of the Ringer's solution at the temperature of T = 37 ±1°C. Metallic ions concentrations were measured with the JY 2000 spectrometer (by Yobin – Yvon) applying the ICP-AES method. The source of induction was plasma torch coupled with frequency generator of 40.68 MHz.

2.6. Surface wettability

To determine the wettability of a surface, contact angle and the surface free energy (SFE) measurements, by means of the Owens-Wendt method, were performed on the selected samples. Contact angle measurements with distilled water (θd) (Merck) and diiodomethane (θw) (Poch SA) were conducted using

drop of liquid with a volume of 1.5 ml. The measurements were performed by applying the SURFTENS UNIVERSAL optical goniometer (OEG) and computer software Surftens 4.5 for analyzing the recorded image of drops. The measurements were carried out at the room temperature ($T = 23 \pm 1°C$) for 60 seconds. Values of the surface free energy (SFE), and their components: a polar and dispersion are given in Table 1.

TABLE 1

The values of SFE and their individual components for measurement liquids

Liquid	Polar component γ_s^p [mJ/m^2]	dispersion component γ_s^d [mJ/m^2]
distilled water	51.0	21.8
diiodomethane	6.7	44.1

2.7. Mechanical properties

Hardness test

Hardness and Young modulus measurements of the deposited layers were conducted with the use of the open platform equipped with a Micro-Combi-Tester (CSM Instruments) using a Vickers indenter. The Oliver & Phar method was applied. The aim of the study was to determine the instrumental hardness versus distance from the surface. Loading and unloading rate was equal to 3000 nm/min, a hold time of the sample at maximum load – 5s. The value of the indenter load was resulting. Microhardness measurements were carried out for the nitrocarburized samples at the ten depths of the penetrator: 500 nm, 1000 nm, 2000 nm, 4000 nm, 6000 nm, 8000 nm, 10000 nm, 12000 nm, 14000 nm and 16000 nm. Additionally, four hardness measurements at depths of 500 nm, 1000 nm, 2000 nm and 4000 nm for samples without the layer at the loading from 25 mN to 1.25 N were carried out.

Scratch test

Scratch tests of the nitrocarburized layers on the 316LVM steel substrate were performed with the use of the open platform equipped with the Micro-Combi-Tester (CSM) in accordance with the PN-EN 1071-3 standard. The study consisted in making the scratch with the use of the penetrator – Rockwell diamond cone – with a gradual increase of the normal force. For the evaluation of scratch resistance a record of the friction force F_t and the penetration depth P_d were used. The tests were performed with the increasing loading force F_c from 0.03 N to 30 N and at the following parameters: loading rate v_s = 10 N/min, the speed of the table v_t = 1 mm/min, the length of the scratch l = 3 mm. For each sample three measurements were carried out.

Statistical analysis

Assumptions of the normality of the distribution (Shapiro-Wilk test) and equality of variance were made. In all cases, these assumptions were met. Therefore, ANOVA has been performed with p = 0.05. Post-hoc analysis has been performed using Tukey test.

3. Results

3.1. Microstructure

The diffusion nitrocarburized layer consisted of two layers, separated by a clear border, of a total thickness of 10 μm (Fig. 1). The outer, thicker layer was composed mainly of a nitrogen austenite γ_N, and the thinner inner layer of a carbon austenite γ_C (Fig. 1). Such structure is caused by differences in diffusion coefficients of carbon and nitrogen in the structure of austenite. Due to the smaller atom diameter, the carbon diffuses deeper than nitrogen. Moreover, the excess of the carbon in the surface layer is pushed by the nitrogen to further parts of the layer (so-called pushing effect), and therefore the greatest concentration is reached in a thin layer (approx. 2 μm) at the substrate [17]. The diffraction pattern shows single peaks from the nitrocarburized austenite γ_{NC}, because the applied CuKa radiation does not reach the deeper localized layer composed only of the carbon austenite γ_C. The information contained in the XRD diffraction pattern is derived from the first, thickest layer composed primarily of nitrogen austenite containing also up to 0.1 wt% of carbon. The diffraction peaks corresponding to the γ austenitic steels structure are also visible in the diffractogram. No carbides or nitrides have been identified in the layer, which means that the given process temperature of 440°C was not exceeded (Fig. 2). According to literature reports [20,21] nitride austenite exhibits a domain structure composed of alternating ferromagnetic and paramagnetic zones. Magnetic transformations in layers may result, among others, from the extent of degradation and the density of misalignment in the austenite structure due to diffusion of nitrogen. The carbon austenite structure does not exhibit ferromagnetic properties, which may result from less deformation of the crystal lattice. The paramagnetism of the nitrocarburized austenite layers is very important for medical applications and especially for implantable materials, however, the magnetic structure of layers of several or more microns does not have

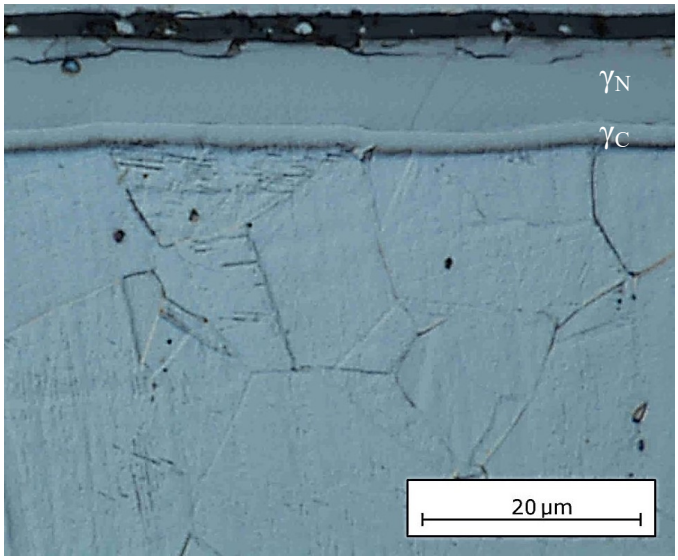

Fig. 1. Microstructure of nitrocarburized layer on austenitic steel

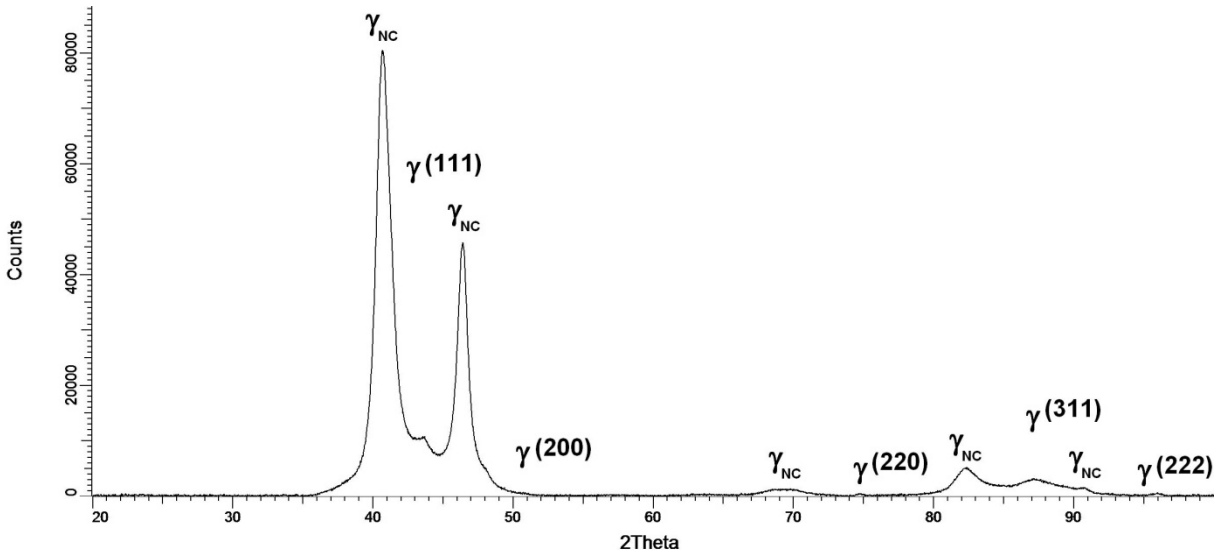

Fig. 2. XRD pattern of nitrocarburized layer on austenitic steel

a significant influence on properties of the whole element. The element with the nitrocarburized austenite still exhibits paramagnetic properties. The presence of a ferromagnetic layer in the tissue environment affects electromagnetic processes, especially for structures exhibiting magnetotropism. These include blood components for which, in consequence, greater tendency to clot formation is observed [3].

3.2. Surface roughness

The results of surface roughness measurements for samples of the all group are shown in Table 2.

TABLE 2

Results of the surface roughness measurements of the 316LVM steel

Group no.	Parameters of surface roughness, µm	
	Ra	*Rz*
	Mechanically polished steel	
I	0.09 ±0.02	0.66 ±0.05
II	0.07 ±0.01	0.43 ±0.05
III	0.05 ±0.02	0.33 ±0.10
	Nitrocarburized steel	
IV	0.16 ±0.01	0.96 ±0.05
V	0.14 ±0.01	0.90 ±0.10
VI	0.14 ±0.01	0.77 ±0.06

Based on the analysis of the measured parameters, it was found that for the samples without the layer, the sterilization process, and exposure to the Ringer's solution caused a decrease of surface roughness *Ra* and *Rz* in relation to the samples after mechanical polishing. In contrast, deposition of the layer increased the *Ra* and *Rz* parameters with reference to the samples without a layer. On the basis of the test, a significant change in the *Ra* and *Rz* parameters was found for the surface with the deposited layer in relation to the polished surface ($p < 0.001$).

Similar values of the Ra and Rz parameters were obtained by other authors [13], who, for the surface of 316L stainless steel with a layer of nitrogen deposited using the potential of the cathode with the active screen, obtained $Ra = 0.12$ µm and $Rz = 0.76$ µm.

3.3. Potentiodynamic study

Examples of the polarization curves in a logarithmic function for the samples of group I, II and III are shown in Fig. 3.

The parameters determined during the corrosion studies of the samples for all the analyzed variants are shown in Table 3.

TABLE 3

Results of potentiodynamic study – mean values

Group no.	E_{corr}, mV	R_p, kΩcm^2	E_b, mV	E_{cp}, mV	E_{tr}, mV
	Mechanically polished steel				
I	–122 ±6	136 ±11	+618 ±5	–47 ±7	—
II	–98 ±14	140 ±5	+1025 ±53	+23 ±6	—
III	–54 ±13	251 ±35	+1052 ±78	+33 ±11	—
	Nitrocarburized steel				
IV	–128 ±29	75 ±14	—	—	+1300 ±43
V	–69 ±11	72 ± 9	—	—	+1425 ±4
VI	–21 ±4	52 ±12	—	—	+1403 ±2

It has been found that, for both mechanically polished samples, as well as the nitrocarburized layers, the sterilization (group II, V) and exposure to the Ringer's solution (group III, VI) significantly increases the corrosion potential E_{corr} ($p = 0.001$). However, for all the polished samples a breakdown potential was recorded, and thus the pitting corrosion was observed. Statistically significant differences in the obtained values were observed between all the tested sample groups ($p < 0.001$). This was confirmed by SEM observations – Fig. 3. The breakdown potential increased with the use of the additional sterilization

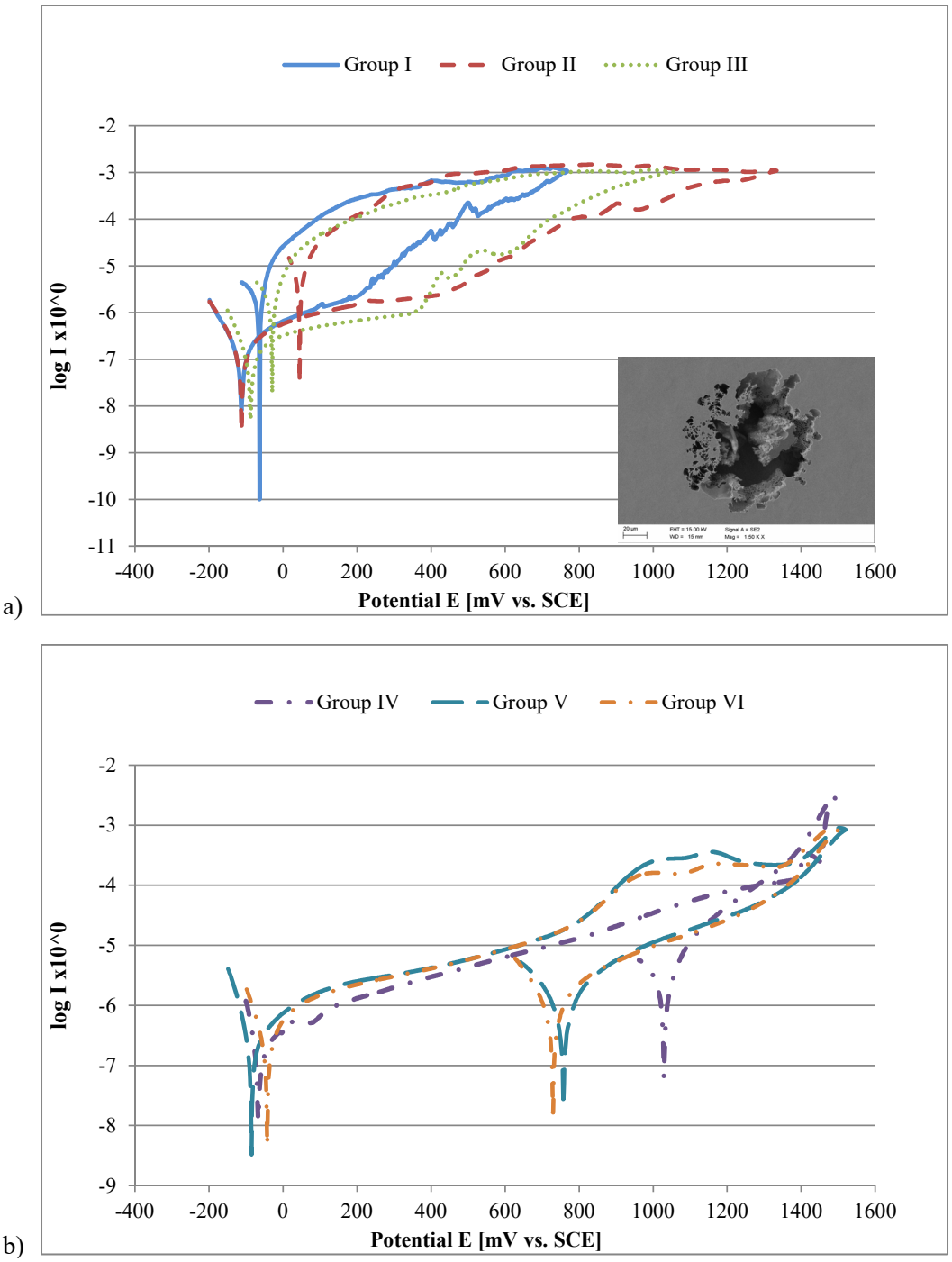

Fig. 3. Examples of polarization curves for groups: a) I, II and III before low temperature glow discharge nitrocarburizing, with corrosion pit – SEM, mag. 1500×, b) III, IV, V after low temperature glow discharge nitrocarburizing

process, and both the sterilization, and the exposure to the Ringer's solution. For the samples with the nitrocarburized layer a transpassivation potential was recorded (group IV, V, VI), which significant increased for the samples sterilized and exposed to the solution ($p = 0.002$), which testifies the positive increase of corrosion resistance in relation to the samples without the layer. However, there was a significant decrease of polarization resistance R_p for the samples with the layer with respect to the mechanically polished ($p = 0.001$), which may be the result of significant development of the surface roughness after the nitrocarburizing process (Table 2).

It can be concluded that the process is beneficial to increase the corrosion resistance compared to the surface only nitrided at 440°C and the chamber pressure – 220 Pa, and the ratio N2/H2 – 1:1 [13]. The study was carried out on 316L stainless steel of ground surface (sandpaper 800), and then nitrogen layer was deposited. It was found for the surface in the initial state was characterized by the occurrence of the breakdown potential equal to 320 mV and the polarization resistance R_p = +231 kΩcm^2. The increase of this value to +1150 mV was obtained for a layer formed on the cathode potential, and to the value of +1250 mV using plasma active screen. In both cases, there was a decrease

of resistance polarization R_p = +91 kΩcm^2 and R_p = +47 kΩcm^2 respectively. Such dependence is also true for the nitrocarburized surfaces.

3.4. Ion release study

The test results of the ions released into the solution after the 28 exposure to the Ringer's solution are presented in Table 4.

TABLE 4

Results of ions release study

Group no.	Released ions, µg/cm^2 (mean value)				
	Fe	Si	Cr	Ni	Mo
I	14.61 ±0.65	9.81 ±0.65	68.18 ±1.30	80.84 ±2.60	157.86 ±1.95
II	13.05 ±0.65	6.62 ±0.65	64.81 ±0.65	78.11 ±1.30	128.96 ±2.60
IV	55.32 ±1.30	5.78 ±0.65	49.03 ±0.65	71.55 ±0.65	99.02 ±0.65
V	51.88 ±0.65	3.57 ±0.65	44.74 ±0.65	64.61 ±0.65	85.78 ±0.65

Assuming the amount of degradation products penetrating into the surrounding tissues as an important criterion demonstrating the biocompatibility, one must conclude that deposition of the nitrocarburized layer has increased protective properties of the material. Studies of chemical composition of the solution in which the samples were held, allowed to identidy the presence of ions of the main alloying elements of the 316LVM steel, such as Cr, Ni, Mo, and Si, but in smaller amounts for the samples with the deposited layer. The highest concentration of ions, for all types of groups was recorded for Mo ions (157.86 µg/cm^2), whereas the lowest concentration was recorded for Si ions (3.57 µg/cm^2). The highest barrier properties were observed for the layers on the samples subjected to sterilization, and exposure to the Ringer's solution, what from the point of view of the presence of the implant in a body, is favorable. It can also be observed that the amount of Fe ions increased for the samples with the layer, which may be caused by creation of unstable form of iron compounds on the surface. Significant differences in values were observed for all the analyzed elements ($p < 0.05$) except for Ni ions between groups I and II ($p = 0.204$).

3.5. Surface wettability

Test results of surface energy and wettability, as well as the examples of drops applied on the surface of the samples subjected to the electrochemical polishing and nitrocarburizing are shown in Figure 4 and Table 5.

TABLE 5

Results of the surface energy calculated on the basis of contact angle measurements – OW method

Group no.	Contact angle, θ [°]		Surface free energy, (SFE), mJ/m^2
	Distilled water	Diiodomethane	
	Mechanically polished steel		
I	90.58 ±2.25	57.62 ±1.68	30.10 ±2.12
II	64.71 ±1.88	36.04 ±1.18	43.65 ±5.31
III	51.13 ±6.56	44.77 ±4.01	48.79 ±4.46
	Nitrocarburized steel		
IV	128.54 ±3.70	64.77 ±3.61	44.77 ±6.23
V	87.93 ±5.38	38.75 ±4.72	41.86 ±5.42
VI	44.95 ±1.41	48.36 ±3.18	53.08 ±2.18

On the basis of the obtained results it was found that from the group of samples without the layer, the highest values of the contact angle were recorded for the mechanically polished surfaces (group I – $p < 0.001$) – average value of the contact angle θ_{sr} was about 90 degrees. Similarly, in the group of samples with the layer, the highest values of contact angle were also recorded for the mechanically polished surfaces (group IV – $p < 0.001$) – the average value of the contact angle θ_{sr} was about 128°. Statistically significant differences occurred in values of contact angle ($p < 0.001$) and SFE between groups I, II and III ($p = 0.004$). This dependence is also maintained for the values of contact angles in groups IV, V and VI ($p < 0.001$), while no such trend was observed between the values of SFE in groups IV, V and VI ($p = 0.164$).

It also can be noted that all the mechanically polished samples, as well as the samples with the layer are hydrophobic, which is advantageous for implants used in orthopedic surgery [22], in contrast to studies carried out by authors of [23], who coated the samples of steel with silica by sol-gel method and observed the increase of wettability for all the tested variants with reference to the polished samples what in the case of the biomaterials used for short term implants is disadvantageous.

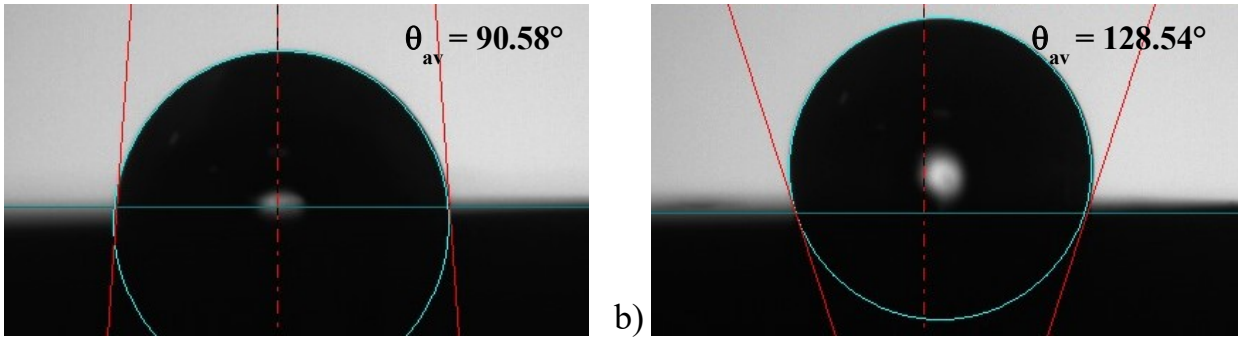

Fig. 4. Examples of measurement of wetting angle, for the groups: a) I, b) IV

In contrast, sterilization, and exposure to the Ringer's solution in each case resulted in a change to a hydrophilic nature of the surface. These values are similar to the obtained by authors of [6], who, for the 316 LVM steel after sterilization and implantation, obtained the values of contact angle from θ_{av} 52.6° to 65.1°.

3.6. Mechanical properties

Hardness test

Test results on hardness and Young's modulus for all the analyzed variants are presented in Table 6.

TABLE 6

Hardness of 316LVM steel surface

	Number of measurement			
	1	2	3	4
	500 nm	1000 nm	2000 nm	4000 nm
	Group I			
Nanohardness H_{IT}, MPa	4966 ±154	4783 ±163	4717 ±158	4081 ±174
Young modulus E, GPa	293 ±17	272 ±19	253 ±16	213 ±15
	Group II			
Nanohardness H_{IT}, MPa	3644 ±182	4054±176	3724 ±187	4256 ±168
Young modulus E, GPa	228 ±15	270±19	237 ±20	238 ±16
	Group III			
Nanohardness H_{IT}, MPa	4009 ±191	4068 ±188	4493 ±194	3960 ±175
Young modulus E, GPa	247 ±21	226 ±17	219 ±19	213 ±18

Taking into account the values of standard deviations for groups I, II and III, slight differences in hardness values were found depending on the depth of penetration. For the depth of 500 nm ($p < 0.001$), 1000 nm ($p = 0.003$), 2000 nm ($p = 0.001$) and 4000 nm – $p > 0.05$ ($p = 0.188$). Therefore, it can be concluded that in contrast to samples from groups V and VI, sterilization and exposure to Ringer's solution slightly change the hardness on the tested depth profile.

Deposition of the nitrocarburized layer resulted in a significant (three times) increase in hardness values with respect to the mechanically polished surface of the 316 LVM steel – Figure 5. It was observed that the highest hardness values were measured for the samples surface exposed to the Ringer's solution H_{IT} = 14068 MPa with reference to samples both before and after the steam sterilization ($p < 0.001$). Significant differences in values were observed at all the tested depths of the profile ($p < 0.05$). The results of hardness obtained at the depth of 12000 nm indicate that the hardness of the substrate was measured – Tables 6-7.

Scratch test

The results of the scratch test are shown in Figures 6-8. On the basis of the obtained results no significant differences were observed in the values of friction force F_t and the depth of penetration of P_d for the samples with the surface layer (group IV) and the samples with the layer subjected to steam sterilization (group V) – Figs. 6 and 7. On the other hand, exposure to the Ringer's solution (VI) caused the increase of the scratch resistance, which has also been confirmed in the nanohardness studies – Table 7.

5. Discussion

Studies conducted in the work indicate beneficial influence of the deposited diffusion layer of nitrocarburized austenite (γ_{NC}) on physicochemical and mechanical properties of the surface. The occurrence of transpassivation potential E_{tr} was recorded indicating the increased resistance to pitting corrosion, in relation

TABLE 7

Hardness and Young modulus of nitrocarburised layers on 316LVM steel

	Number of measurement									
	1	2	3	4	5	6	7	8	9	10
	500 nm	1000 nm	2000 nm	4000 nm	6000 nm	8000 nm	10000 nm	12000 nm	14000 nm	16000 nm
	Group IV									
Nanohardness H_{IT}, MPa	13414 ±192	12794±165	12060±178	8071±194	6171±205	5865±188	4782±196	4780±182	4559±204	4501±196
Young modulus E, GPa	229 ±18	230 ±16	226 ±21	187 ±22	178 ±18	178 ±17	164 ±19	169 ±22	162 ±23	161 ±15
	Group V									
Nanohardness H_{IT}, MPa	10581±171	11943±184	10057±186	7062±192	5502±196	4414±201	4352±176	4397±183	4194±191	3913±159
Young modulus E, GPa	216 ±19	218 ±17	209 ±16	184 ±20	167 ±19	154 ±22	156 ±25	153 ±14	148 ±17	149 ±18
	Group VI									
Nanohardness H_{IT}, MPa	14068±203	15085±200	13292±189	6588±175	5463±163	4720±169	4290±170	4117±197	4125±192	4021±206
Young modulus E, GPa	273 ±17	260 ±17	219 ±20	202 ±21	168 ±19	172 ±16	170 ±14	168 ±18	169 ±20	170 ±18

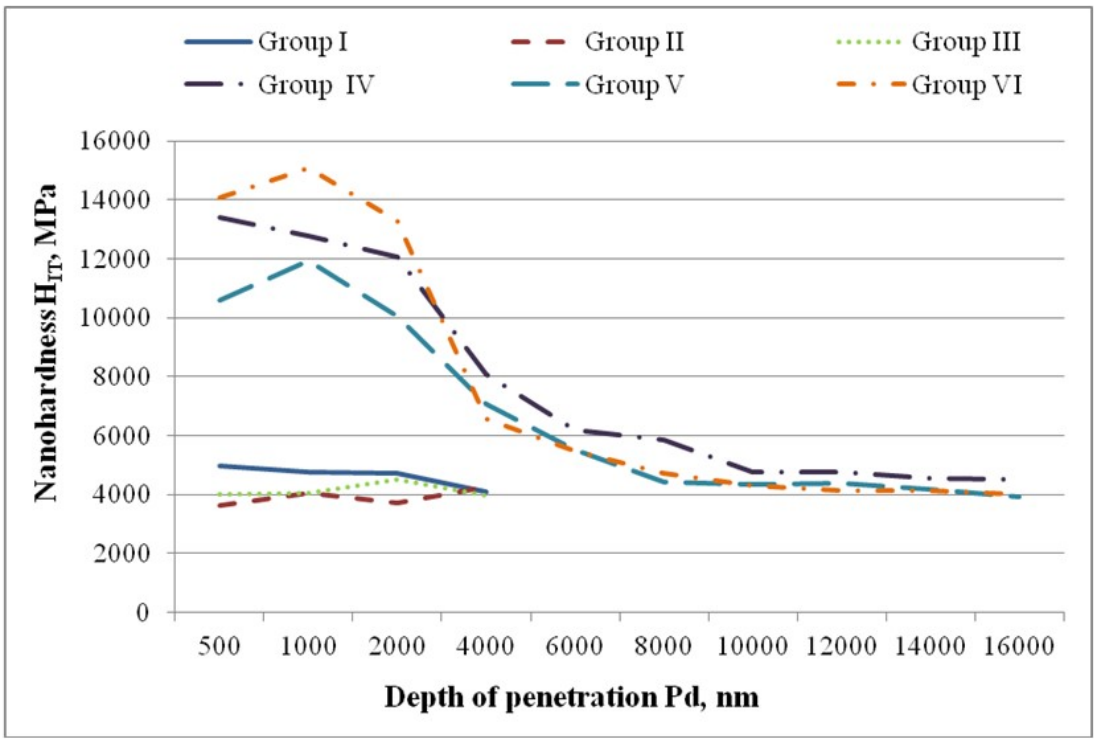

Fig. 5. Nanohardness in a function of penetration depth

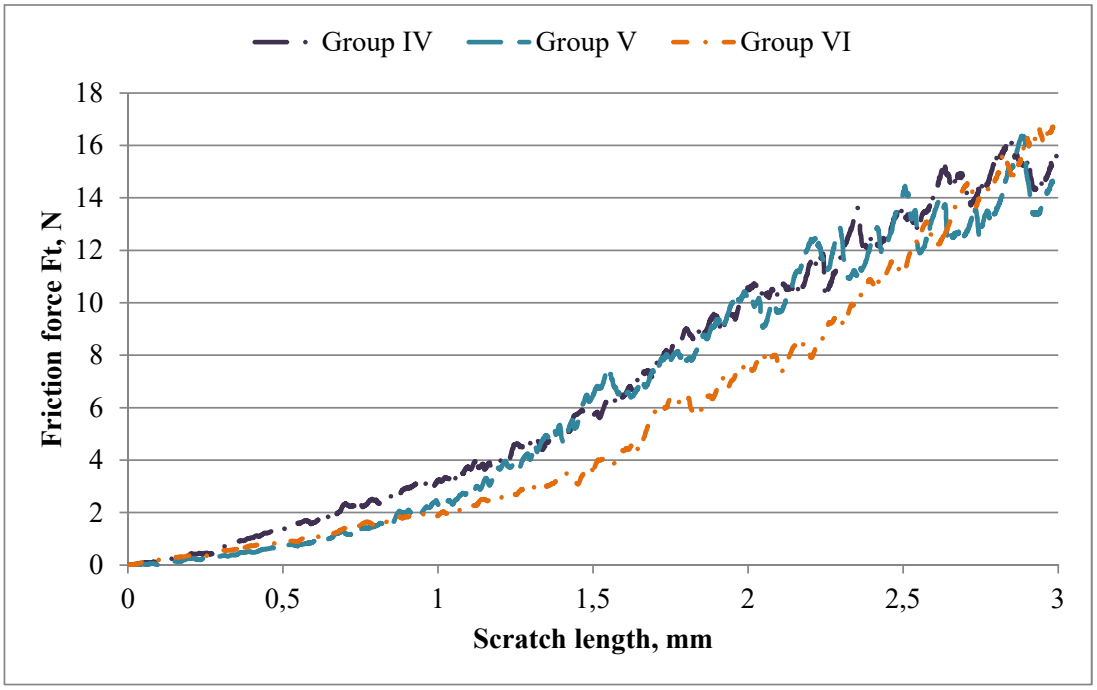

Fig. 6. Example relation between friction force and the scratch length

to the polished surface, for which the breakdown potential E_b was recorded. Similar results were find in work of other authors [6], who studied 316 LVM stainless steel explants and obtained the breakdown potential E_b from 1089 mV to 1219 mV, while polarization resistance R_p from 215 kΩ·cm^2 to 283 kΩ·cm^2. These values are similar for samples obtained from the group III (after sterilization, and exposure to the Ringer's solution). Additionally, the decrease of ions penetration (of the main alloying elements of the 316LVM steel) was observed, thereby reducing the possible metalosis. One may conclude that after the surface modification the steel will be characterized by increased biocompatibility. Deposition of the layer also caused the increase of surface roughness and decrease the surface wettability. According to the results obtained by the authors of [24] it can be concluded that the wettability of the surface is not always dependent on the morphology and surface topography.

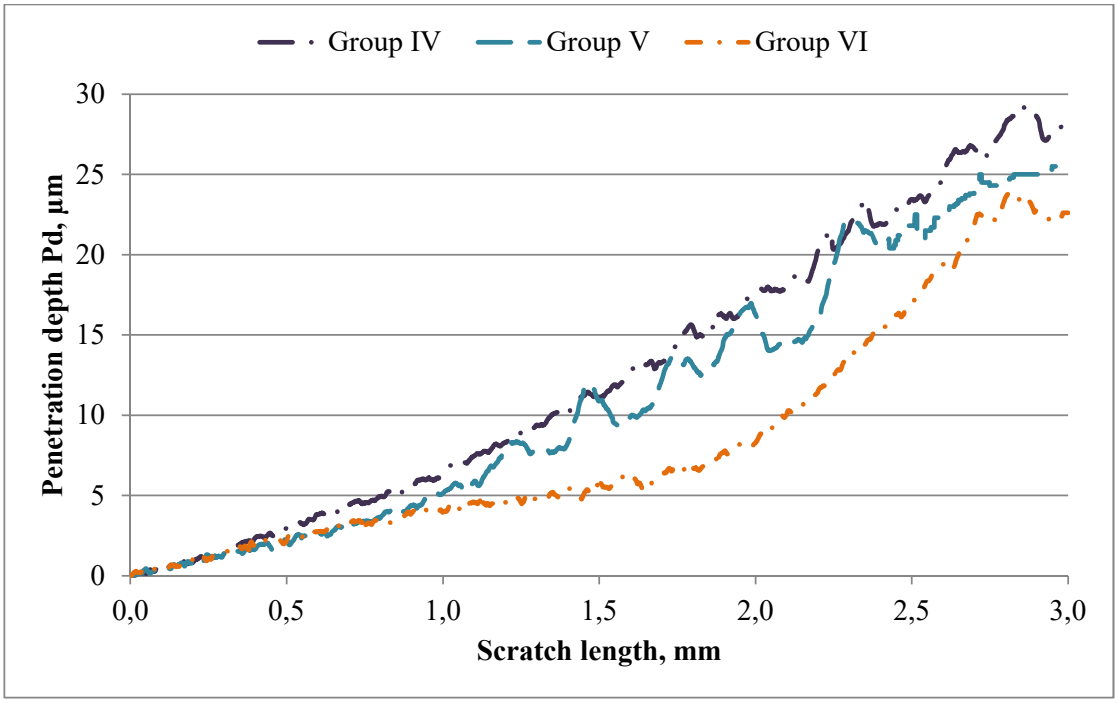

Fig. 7. Example relation between penetration depth in the function of the scratch length

Lower wettability is beneficial for short term implants for which no tissue ingrowth should be observed, because it makes them difficult to remove after a given time of implantation. Taking into account the implantation technique and combining parts of implants, the appropriate surface hardness is important. The proposed type of surface treatment contributed to the increase of hardness. It was also found that the hardness decreases from the surface to the substrate. This may indicate deformability of the layer, which is important for the implant in case of fitting to an anatomical curvature of treated deformation or fracture. Jiang Y et al. [25] also conducted hardness testing of nitrocarburized layers deposited on the substrate of the Q235 steel. The obtained hardness values were equal to H_{IT} = 4760 MPa. These values are much lower than those obtained in the work. However, Lee I and Barua A [26] reported similar hardness of the nitrocarburized layer deposited on the substrate of the 316L steel, while Liu at al [27] obtained for the carbonitrided 316 LVM steel increase of microhardness from 2.7 GPa for the polished surface up to 13.3 GPa for the samples with the layer. This value is close to one obtained in the work for the nitrocarburized surface (group IV). The applied steam sterilization performed for both polished and nitrocarburized surface caused the decrease of surface roughness, and the increase of transpassivation potential. In addition, the exposure to the Ringer's solution increased the scratch resistance, as confirmed by microhardness tests, and increased the corrosion potential E_{cor}. For this group of samples the smallest amount of metal ions penetrating to the solution was also observed. In conclusion it can be stated that the sterilization and the exposure to the Ringer's solution of the nitrocarburized 316 LVM steel does not decrease its biocompatibility.

6. Conclusion

On the basis of the obtained results the following can be stated:

- deposition of the nitrocarburized layer increased the surface roughness, surface hardness the contact angle, and corrosion resistance with respect to the polished surfaces,
- for both mechanically polished samples, as well as the nitrocarburized layers, the sterilization (group II, V) and exposure to the Ringer's solution (group III, VI) increases the corrosion potential E_{corr}. The breakdown potential increased with the use of the additional sterilization process, and both the sterilization, and the exposure to the Ringer's solution
- the highest hardness values were measured for the samples exposed to the Ringer's solution with reference to samples both before and after the steam sterilization,
- exposure to the Ringer's solution (VI) caused the increase of the scratch resistance, which has also been confirmed in the nanohardness studies,
- the nitrocarburized layer is a barrier against the release of ions to the solution, but it can also be observed that the amount of Fe ions increased for the samples with the layer, which may be caused by creation of unstable form of iron compounds on the surface.

Summing up the results of the research it can be concluded that the proposed method of surface modification contributed to the improvement of mechanical and physicochemical properties. This involves the possibility of a wider use of 316 LVM steel for implants in bone surgery.

REFERENCES

[1] K.H. Lo, C.H. Shek, Mat. Sci. Eng. R. **65**, 39-104 (2009).

[2] P. Boillot, J. Peultier, Procedia Engineering **83**, 309-321 (2014).

[3] J. Marciniak, Biomateriały. Wydawnictwo Politechniki Śląskiej, Gliwice 2013 (in polish).

[4] C.X. Li, T. Bell, Corros. Sci. **46**, 1527-1547 (2004).

[5] A. Krauze, A. Zębowicz, J. Marciniak, J. Mater. Process. Tech. **162-163**, 209-214 (2005).

[6] A. Kajzer, W. Kajzer, J. Dzielicki, D. Matejczyk, Acta Bioeng. Biomech. **17**, 2, 35-44 (2015).

[7] W. Walke, Z. Paszenda, T. Pustelny, Z. Opilski, S. Drewniak, M. Kościelniak-Ziemniak, M. Basiaga, Mat. Sci. and Eng. C **63**, 155-163 (2016).

[8] W. Walke, Z. Paszenda, M. Basiaga, P. Karasiński, M. Kaczmarek, EIS study of SiO2 Oxide Film on 316L stainless steel for cardiac implants. Information Technologies in Biomedicine. Advances in Intelligent Systems and Computing 284, Springer (2014).

[9] W. Kajzer, A. Kajzer, M. Grygiel-Pradelok, A. Zębowicz, B. Zębowicz, Evaluation of physicochemical properties of TiO_2 layer on AISI 316 LVM stainless steel intented for urology. Advances in Intelligent Systems and Computing 471, Springer International Publishing (2016).

[10] L. Orellana-Martínez, F.J. Pérez, C. Gómez, Surf. Coat. Tech. **200**, 1609-1615 (2005).

[11] A. Kajzer, O. Grzeszczuk, W. Kajzer, K. Nowińska, M. Kaczmarek, M. Tarnowski, T. Wierzchoń, Acta Bioeng. Biomech. **19**, 4, 181-188 (2017).

[12] J. Baranowska, B. Arnold, Surf. Coat. Tech. **200**, 6623-6628 (2006).

[13] T. Borowski, B. Adamczyk-Cieślak, A. Brojanowska, K. Kulikowski, T. Wierzchoń, Mat. Sci. Medziagotyra. **21**, 3, 376-381 (2015).

[14] Z. Cheng, C.X. Li, H. Dong, T. Bell, Surf. Coat. Tech. **191**, 195-200 (2005).

[15] L. Shen, L. Wang, J. Xu, Surf. Coat. Tech. **228**, 456-459 (2013).

[16] R.R.M. de Sousa, F.O. de Araújo, L.C. Gontijo, J.A.P. da Costa, Jr.C. Alves, Vacuum **86**, 2048-2053 (2012).

[17] M. Ossowski, T. Borowski, M. Tarnowski, T. Wierzchoń, Mat. Sci. Medziagotyra. **22**, 1, 25-30 (2016).

[18] M. Basiaga, W. Walke, M. Staszuk, W. Kajzer, A. Kajzer, K. Nowińska, Arch. Civ. Mech. Eng. **17**, 32-42 (2017).

[19] T. Czerwiec, H. He, G. Marcos, T. Thiriet, S. Weber, H. Michel, Plasma Process Polym. **6**, 401-409 (2009).

[20] C. Blawert, H. Kalvelage, B.L Mordike, et al, Surf. Coat. Tech. **136**, 181-187 (2001).

[21] M.F. Fewell, D.R.G. Mitchell, et al, Surf. Coat. Tech. **131**, 300-306 (2000).

[22] L.C. Xu, Biomaterials. **28**, 3273-3283 (2007).

[23] M. Houmarda, E.H.M. Nunesb, D.C.L. Vasconcelosb, G. Berthoméc, J.C. Joudc, M. Langletd, W.L. Vasconcelosba, Appl. Surf. Sci. **289**, 218-223 (2014).

[24] E. Sobolewska, B. Frączak, S. Błażewicz, K. Seńko, M. Lipski, Protet. Stomatol. **6**, 401-406 (2009).

[25] Y. Jiang, Y. Bao, K. Yang, Surf. Coat. Tech. **269**, 324-328 (2015).

[26] I. Lee, A. Barua, Surf. Coat. Tech. **307**, 1045-1052 (2016).

[27] J. Liu, H. Dong, J. Buhagiar, C.F. Song, B.J. Yu, L.M. Qian, Z.R. Zhou, Wear. **271**, 1490-1496 (2011).